A Comparative Analysis of Force Fields of Drug-Like Molecules: Omeprazole, Favipiravir and Amoxicillin by using Bonded and Non-Bonded Potential Distributions

P. K. Yadav and T. R. Lamichhane

Journal of Nepal Physical Society

Volume 9, Issue 1, June 2023

ISSN: 2392-473X (Print), 2738-9537 (Online)

JNPS, **9** (1): 58-72 (2023)

DOI: https://doi.org/10.3126/jnphyssoc.v9i1.57599

Published by:

Nepal Physical Society
P.O. Box: 2934
Tri-Chandra Campus
Kathmandu, Nepal
Email: nps.editor@gmail.com

JNPS 9 (1): 58-72 (2023)
ISSN: 2392-473X (Print), 2738-9537 (Online)
Research Article *© Nepal Physical Society*
DOI: https://doi.org/10.3126/jnphyssoc.v9i1.57599

A Comparative Analysis of Force Fields of Drug-Like Molecules: Omeprazole, Favipiravir and Amoxicillin by using Bonded and Non-Bonded Potential Distributions

P. K. Yadav and T. R. Lamichhane*
Central Department of Physics, Tribhuvan University, Kathmandu, Nepal
*Correspondence Email: tika.lamichhane@cdp.tu.edu.np

Received: *10th May, 2023;* ***Revised:*** *31st May, 2023;* ***Accepted:*** *28th June, 2023*

ABSTRACT

This research aims to compare and analyze the force field parameters of drug-like compounds generated by the online servers CGenFF, SwissParam, and LigParGen. CHARMM27, OPLS-AA, and CHARMM36 force fields of amoxicillin, favipiravir, and omeprazole have been examined by bonded and non-bonded energy distributions of the potential function. The local terms of the force field function are bond length, bond angle, and dihedral potentials, while the non-local terms are van der Waals and pairwise electrostatic interactions. The parabolic curves of bond length potential appear to internally bend because of the larger values of force constants. The bond length and angle energies are lowest at reference values for each of the corresponding atom pairs in the molecules. The higher values of the bending force constant positively deflect the sinusoidal curve from the equilibrium position according to the dihedral angle energy distribution. The Lennard-Jones interaction exhibits the same repellent nature at closer ranges and the same attracting nature at farther ranges whereas a mildly differentiated interaction is seen at the intermediate state as a result of changing well-depth parameters. Depending on the size of the optimized partial charges, it is discovered in electrostatic interaction that the distributions of end-to-end lengths of identical atom pairs are more exponentially skewed from one another. The main cause of inconsistency in the results of MD simulations for the same protein-ligand system is due to the shifted topology and parameters.

Keywords: Bonded and non-bonded energy; CHARMM27; CHARMM36; Drug-like molecules; Force field potential function; OPLS-AA.

INTRODUCTION

Small drug-like molecules for force field analysis typically have simple structures and are composed of fewer atoms. Examples include small organic molecules like aspirin or caffeine. These molecules are often studied using bonded force fields, which can accurately predict their behavior and interactions with other molecules. When it comes to analyzing the force fields of drug-like molecules, there are several different methods and approaches that can be taken. Some of the most commonly used techniques include molecular dynamics simulations, quantum mechanical calculations, and empirical force field-based methods. Each of these approaches has its own strengths and weaknesses, and understanding how they compare and contrast with one another is critical for accurately predicting the behavior of drug molecules in biological systems. In this comparative analysis, we'll explore some of the key differences between these different methods and investigate which ones might be best suited for different types of drug-like molecules and therapeutic applications. Biomolecular modeling is driven by designing structures, predicting physicochemical properties, and analyzing interactions with receptor systems. It is frequently difficult to determine which method would provide the most accurate predictions for the target system without thoroughly evaluating all available methods. Such comparative evaluations are uncommon and difficult to carry out because no single group is familiar with or has access to all

relevant methods. The experimental data sets are not widely available enough to allow for prospective evaluations. Because of recent advancements in computer hardware, algorithms, and force field parameterization, molecular dynamics (MD) simulations are widely used [1]. To make reliable predictions, the methods, which are mostly based on molecular mechanics (MM), require force fields (FFs) that accurately describe the interactions. Accurate force fields (FFs) used in molecular modeling research have the potential to gain insight into the structure, dynamics, and functional characteristics of the systems [2].

The biochemical processes are influenced by small organic molecules that interact with proteins called ligands which are primarily termed drugs [3] . The mechanism of action of drugs, their interaction, and complex formation is the major query of understanding. We have chosen omeprazole, favipiravir, and amoxicillin as drug-like molecules to study the force field under SwissParam, LigParGen, and CGenFF servers. The SwissParam was developed for CHARMM22/27, CGenFF is compatible with CHARMM36 FF and LigParGen is compatible with OPLS-AA. The LigParGen web server provides an intuitive interface for the purpose of generating OPLS-AA/1.14*CM1A(-LBCC) force field parameters for organic ligands in the formats of widely used molecular dynamics and Monte Carlo simulation packages. The OPLS-AA force field was initially designed and parameterized to simulate the experimental vaporization temperatures and densities of small organic molecules, and it was later expanded to incorporate proteins and nucleic acids [4]. It has been found that 1.20*CM5 [5] and 1.14*CM1A [6] charges are the most accurate for OPLS-AA to reproduce experimental HFEs. The accuracy of 1.14*CM1A charges is further improved using localized bond charge corrections (LBCC), making 1.14*CM1A-LBCC [7] the best QM charge model currently available at a comparable computational cost to CM1A charges. For the prediction of the hydration free energies of typical small organic molecules, current force fields are believed to be accurate to 1-2.5 kcal/mol [8], and techniques based on traditional all-atom MD simulations can offer accurate predictions for hydration free energies [9].

Because of the magnitude of the chemical space, the parametrization of a small molecule remains an open problem. The LigParGen web server [10] provides an intuitive interface for generating force field parameters for organic ligands. This web server does not require a login and is available to all at jorgensenresearch.com/ligpargen. The latest advancements in force field parametrization and algorithm development have made a significant contribution to the vast number of applications of molecular simulations in various sectors of biomolecular studies [11]. The molecular mechanics (MM) force fields (FF) accurately describe the interactions and provide a reasonable prediction. The LigParGen server automatically and simply assigns the parameters and generates the files required for the calculation. Standard parameters such as partial charges and FF parameters are already missing from the small molecule. This server's force field calculations require the addition of RTF (topology), PRM (parameter), and PDB (coordinate) files.

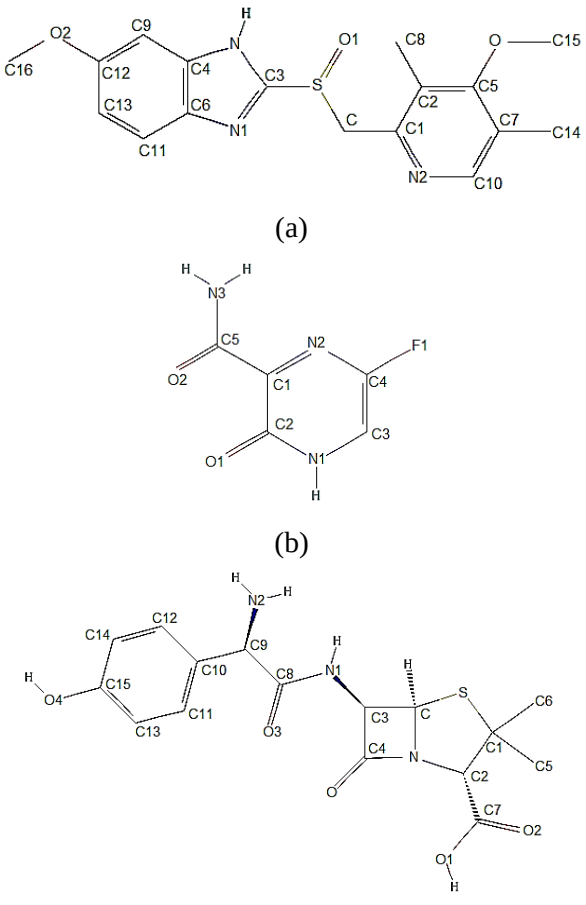

Fig. 1: Chemical structure of (a) omeprazole, (b) favipiravir, and (c) amoxicillin molecules.

The FF parameters for MD simulations are generated by different online servers like LiGparGen, SwissParam and CGenFF in terms of

different file formats. The docking or Poisson–Boltzmann calculations can use a single PQR file format which is generated by these servers. The LigParGen web server is a powerful, open-source, and completely free tool for generating OPLS-AA parameters for organic molecules. In addition, LigParGen provides an interface for creating optimized potentials for liquid simulations. The parameters of energy functions are primarily derived from quantum mechanical calculations and various physics and chemistry experiments. A force field parameter file contains all of the numerical constants required to evaluate forces and energies for a given set of atomic coordinates and structure file [12]. The illustrations of the preparation of protein-ligand systems or ligand-water boxes for molecular dynamics (MD) simulations are included on LigParGen. The well-known programs such as NAMD, OpenMM, CHARMM, and GROMACS [13] accept the output files which are formatted for direct use.

SwissParam is a force-field generation program that generates Merck molecular force field (MMFF) topologies and parameters that are compatible with CHARMM force fields. For quick calculations like docking and minimization, it was developed. Despite being used in numerous MD studies, it might not be suitable for prolonged MD simulations [14]. SwissParam offers topology and parameter files for small organic molecules compatible with the CHARMM all atoms force field. The data for this server is provided by MMFF [15], the molecular modeling group, SIB, who also created and maintains the server. Only the harmonic portion of the bond, the angle, and the improper terms are obtained using the charges from MMFF. The van der Waals parameters are provided by the closest atom type in CHARMM27. All the hydrogen atoms of the molecule must be contained in .mol2 files submitted to SwissParam. The .mol2 file format can be generated by converting another file format using UCSF Chimera [16]or Open Babel tool [17]. For the description of a small molecule to be docked the docking software EADDOCK2 and EADOCK DSS [18] use the topology and parameters generated by SwissParam. Academic users can use SwissParam freely at www.swissparam.ch.

An arbitrary drug-like molecule can have its atom types, parameters, and charges assigned using the CHARMM general force field (CGenFF). The bonded parameters are assigned based on the substitution of atom types in the definition of the desired parameters. In order to assign the charges, an extended bond-charge increment scheme is used. The CGenFF output files that are linked to the partial charges and parameters also contain the penalty scores. When the penalty score is under 10, the analogy is considered to be fair. Scores of penalties between 10 and 50 are associated with some basic analogy validation, while scores higher than 50 demand extensive optimization with a subpar analogy. The combination of all the small molecules into one force field is the starting point of CGenFF. It is used to calculate the well-validated Lennard-Jones parameters, standardized charges for some chemical groups, and bonded parameters. Analogy is used to create the parameters, which are then optimized [19].

A more optimized force field allows for more realistic system interaction. To create force fields for new molecules, CHARMM sets of optimized energy functions are used. CGenFF was created using the ParamChem project. CGenFF contains many common biological groups, with a strong emphasis on heterocyclic rings [20]. The LigParGen generates three distinct output files, whereas CGenFF generates a stream file for each ligand. The force field free energy method is used to investigate phenomena in complex biological and material systems [21]. Bonded vibrations and electrostatic interaction approximation are explained by harmonic terms and fixed-point charges, respectively [22]. All system components must be accurately parametrized by a force field. The primary goal of our research is to observe and analyze variations in the energy profiles of the parameters provided by these servers for bond length, bond angle, dihedral angle, Lennard-Jones potential, and Coulomb potential. Bond stretching refers to the forces that exist between two covalently bonded atoms [23]. Angle bending is the force produced by the deformation of the valence angles between three covalently bonded atoms [24]. Torsional terms can explain the rotational barriers between four bonded atoms [25], which are less powerful than bond stretching and angle bending terms. A simple Lennard-Jones potential [26] made up of repulsion and attraction terms explains Van der Waals interactions between atoms that are not covalently bonded to one another. The electrostatic potential explains the interaction of partial charges [27].

Force Field Potential Functions

The additive principle expresses potential energy as the sum of local and non-local terms. The bond length, bond angle, dihedral, Urey-Bradley, and

improper dihedral potentials are included in local terms and van der Waals and pairwise electrostatic interactions are included in non-local energy terms. The CHARMM force field in the functional form [28] is expressed as Equation 1 or 2 and 3.

$$U_{total} = U_{bonded} + U_{non-bonded} \quad \text{.....(1)}$$

where U_{bonded} includes bonded terms (covalently linked atoms) which are also called intramolecular potential and $U_{non-bonded}$ includes non-bonded terms (long-range electrostatic and van der Walls forces) which are also called intermolecular potential energy.

$$U_{bonded} = \sum_{bonds} k_x(x - x_0)^2 + \sum_{bond\ angles} k_\beta(\beta - \beta_0)^2 + \sum_{dihedrals} k_\alpha[1 + \cos(n\alpha - \delta)] + \sum_{Urey-Bradley} k_f(f - f_0)^2 + \sum_{Impropers} k_\psi(\psi - \psi_0)^2 \quad \text{.....(2)}$$

where x is the bond length, x_0 is the equilibrium bond length, β is an acute angle, β_0 is the equilibrium bond angle, α is a torsional angle, k_x is bonding force constant, k_α is bending force constant, k_f is the Urey-Bradley force constant, k_ψ is the potential stiffness constant, f is the distance between the two external atoms forming the angle, δ is phase angle in cosine series and n is dihedral multiplicity. The average interaction of each of the bonded atoms is found from crystallographic data within such a minimum error and depicted as x_0, β_0, f_0, and ψ_0.

Similarly, $U_{non-bonded}$ is the sum of Coulomb potential (electrostatic interaction) and Lennard Jones potential (van der Waals interaction) which is expressed in Equation 3.

$$U_{non-bonded} = \sum_{nonbonded\ atom\ pairs} \left(4\epsilon_{ij} \left[\left(\frac{\sigma_{ij}}{r_{ij}} \right)^{12} - \left(\frac{\sigma_{ij}}{r_{ij}} \right)^{6} \right] + \frac{K q_i q_j}{\epsilon_{ij} r_{ij}} \right) \quad \text{.....(3)}$$

where q_i and q_j are the partial atomic charges of atom i and j respectively, ϵ_{ij} is the well depth, σ_{ij} is the radius in the Lennard-Jones 6-12 terms used to treat the van der Waals interaction and r_{ij} is the distance between i and j atoms. The existing CGenFF parameters are comparable to parameters developed for a small set of molecules using ffTK [29].

The "drug-like molecules in a biological environment" is targeted by the principle of CGenFF and general Amber force field (GAFF). Several tools are created in response to various difficulties in order to assign missing parameters directly from analogies to ones that already exist. ParamChem and MATCH are the tools for the CHARMM force field. By using existing CHARMM atom types as analogies, SwissParam assigns van der Waals terms. By analogy, the Merck molecular force field's charges, bonds, angles, dihedrals, and impropers are taken and converted into the CHARMM format. The distribution of CGenFF enables the creation of an extensive parametrization tool that can generate a complete set of CHARMM/CGenFF-compatible parameters.

Atomic interaction is described in the CHARMM force field using harmonic potentials for the unnecessary internal coordinates defined by bonds, bond angles, and dihedral impropers [30]. Martin Karplus's lab at Harvard University is creating CHARMM force field, a multipurpose simulation program with a focus on proteins. Bonded terms provide a quantum mechanical description of the shared electron orbitals that create chemical bonds as well as the internal degree of freedom of nearby molecules. The energy needed to scissor the angle away from its equilibrium value is explained by the bonded terms. Due to the minimal changes from the equilibrium distance, the harmonic approximation is valid for biological application. A full 360°of rotation about a bond at normal temperature is found in dihedral energy. The location of atoms and the approximation used in calculating the forces such as the non-bonded cutoff distance are the key factors on which the contents of a non-bonded atom depend [31]. The CHARMM related force fields are united atom CHARMM19 [32], all atom CHARMM22 [33], CHARMM27 [34], and CHARMM36.

METHODOLOGY

The SwissParam, LigParGen, and CGenFF online servers are used to predict the force field parameters of small drug-like molecules. The molecules such as omeprazole ($C_{17}H_{19}N_3O_3S$, CID 4594), favipiravir ($C_5H_4FN_3O_2$, CID 492405), and amoxicillin ($C_{16}H_{19}N_3O_5S$, CID 33613) having aromatic rings and a variety of functional groups

were chosen for the force field analysis. Covering chemical space, training data, and strategies for parameter improvement are important force field development strategies [35]. The initial structures of these molecules were obtained in SDF format from the PubChem database. Using the Open Babel software, the SDF format was converted to PDB format. These molecules were optimized and H-atoms were added and saved in .mol2 format using UCSF Chimera before uploading to the parameter generation server. The generated .mol2 format was uploaded to CGenFF and Swissparam and PDB/smile format was uploaded to LigParGen. The identical name is given to the atoms obtained under SwissParam, LigParGen, and CGenFF programs. The output files as .rtf and .par of SwissParam, .rtf and .prm of LigParGen, and .str of CGenFF program were used to draw the energy profiles of the potential function for these molecules using Matplotlib version 3.6.2 in combination with Python 3.10.6. This method was revised at least three times to validate the results. The bonded and non-bonded parameters, including partial atomic charges and effective torsional potentials, are calculated using quantum chemical calculations in accordance with the CHARMM protocol. The generated parameters of the potential energy function of small drug-like molecules are suitable for use in computational simulation tasks. The parameter file includes references to the specific equilibrium bond lengths and angles, bond and angle force constants, dihedrals, and impropers. Even after the automated process, additional parameter optimization may be required [36]. Intermolecular optimization is used to obtain partial atomic charges and van der Waals parameters. The intramolecular optimization results in bond, angle, torsion, and improper parameters. We have primarily concentrated on analyzing changes in bond length, bond angle, dihedral angles, Lennard-Jones, and electrostatic interactions because they are the essential components of the force field function. We have neglected the study of the Urey-Bradley potential because SwissParam, LigParGen, and CGenFF servers do not provide parameters for this potential. If the intermolecular and intramolecular charges are less than the convergence criteria, then the parameters are said to be completely optimized. A stream file is automatically generated after submitting the optimized structure to CGenFF. The stream file contains information on the topology and parameters of the submitted molecule preserving the integrity of the original structures. Using the correct .mol2 format as input, the CGenFF program predicts the reliable CHARMM force field parameters. Based on the .mol2 input format, the atom types, partial atomic charges, and guessed parameters assigned with penalty scores can be retrieved automatically. These parameters can be used to yield well-fitted force field geometries. Though CGenFF generates an optimized set of parameters, the submitted molecule requires better optimization in order to get lower penalty scores. Three different molecular structure input formats, including MOL files, SMILES codes, and PDB, are supported by the LigParGen server. For the purpose of optimizing molecule structural properties, BOSS uses the Broyden-Fletcher-Goldfarb-Shanno variable metric algorithm [37]. The SMILES code can be copied for the structure submission and the "make SMILES" button assists in converting the 2D structures produced by JSME. If two total charges match, coordinate and parameter files in all the different formats are generated and displayed on the LigParGen output page [38]. The drug-like molecules' SMILES codes are uploaded one at a time to the LigParGen server. In order to obtain PDB, PRM, and RTF files, the zero optimization iterations and 1.14*CM1A charge model were first chosen. The amount of optimization steps and the size of the molecule are the two factors that affect processing time the most. For a small or medium molecule, the computational time is typically less than 5 seconds, and depending on the size and quality of the input structure, the computational time during the submission of the structure optimization can range from 30-45 seconds. The optimization time for SMILES input is reduced due to the generation of structures close to the equilibrium conformation.

RESULTS AND DISCUSSION

Bond Length Energy

Bond length energy controls the covalent bond lengths based on Hook's law (harmonic potential). This energy became low at the equilibrium bond lengths for the respective atom pairs for all selected molecules. The plots for CHARMM27 parameters of the important bonded atom pairs N1-C3 of omeprazole, C3-C4 of favipiravir, and CHARMM36 parameters of C10-C11 of amoxicillin (see Table 1) were found more bending parabolically inside due to the higher values of force constants as shown in Figure 1-a, b, and c.

Table 1: Parameters for bond length interactions under CHARMM27, OPLS-AA, and CHARMM36 FFs

Molecules	Atoms	CHARMM27		OPLS-AA		CHARMM36	
		k_x (kcal/mol/Å^2)	x_0 (Å)	k_x (kcal/mol/Å^2)	x_0 (Å)	k_x (kcal/mol/Å^2)	x_0 (Å)
Omeprazole	N1-C3	599.191	1.313	488.000	1.335	400.000	1.320
Favipiravir	C3-C4	684.039	1.333	549.000	1.340	394.000	1.375
Amoxicillin	C10-C11	401.068	1.374	469.000	1.400	305.000	1.375

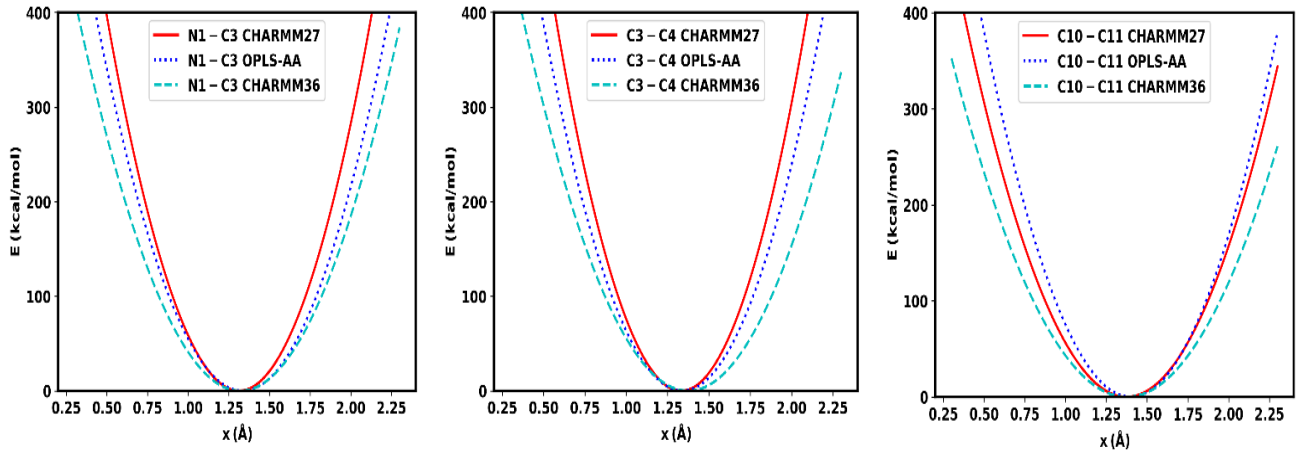

(a) Omeprazole (b) Favipiravir (c) Amoxicillin

Fig. 2: Harmonic bond length potentials of the form $k_x(x-x_0)^2$ for the atom pairs of (a) omeprazole, (b) favipiravir, and (c) amoxicillin for three different force fields: CHARMM27 (red), OPLS-AA (blue, dotted), and CHARMM36 (cyan, dotted).

The frequency of bond length fluctuation is given by $\omega^2 = \frac{2kx}{m}$, where m is the mass of the bonded particle. For smaller bond length deformation (<10%), the harmonic potential is only sufficient for small deviation from equilibrium values [39]. Due to the atom dissociation and no longer interaction, this potential is not valid for larger deviations from equilibrium values. Hence, when distances are increased from equilibrium, the energy levels become off rather than increment [40].

For macromolecules, the minute variations between the reference values typically matter. The simplest molecular mechanics formulation, Hook's law, is used to model harmonic potential for bonded deformations. Since there is no bond breaking in these harmonic functions, no chemical process can be studied. The deformation energy is found very large for very small interaction distances. The parabolic potential with a well-shaped curve is found for the smaller separation. Taylor expansion is used to describe the shape of the energy curve. The cubic terms are neglected because the change in curvature causes bond stretching [41]. A potential well stretching over a wide range of distances is reproduced by Morse potentials and at longer distances, it becomes zero. When the initial geometry has a large bond length, the Morse potential is found slow in bringing atoms to equilibrium bond length [42]. Stretching and bending energies both contribute significantly to the system's overall energy.

Bond Angle Energy

Bond angle energy became low at the equilibrium bond angles for the selected atom pairs. The energy profiles of bond angle plots for CHARMM27, OPLS-AA, and CHARMM36 parameters of important atom groups N-C4-C6 of omeprazole, O1-C2-N1 of favipiravir, and C-N-C2 of amoxicillin (see Table 2) were found more bending parabolically inside in Figure 3-a, b, and c due to higher values of force constant.

Table 2: Parameters for bond angle interactions under CHARMM27, OPLS-AA, and CHARMM36 program

Molecules	Atoms	CHARMM27		OPLS-AA		CHARMM36	
		k_β (kcal/mol/rad^2)	β_0 (radian)	k_β (kcal/mol/rad^2)	β_0 (radian)	k_β (kcal/mol/rad^2)	β_0 (radian)
Omeprazole	N-C4-C6	58.508	107.255	70.000	108.700	100.000	105.700
Favipiravir	O1-C2-N1	65.273	127.152	160.000	120.600	130.000	119.400
Amoxicillin	C-N-C2	69.087	119.679	50.000	126.000	34.000	125.300

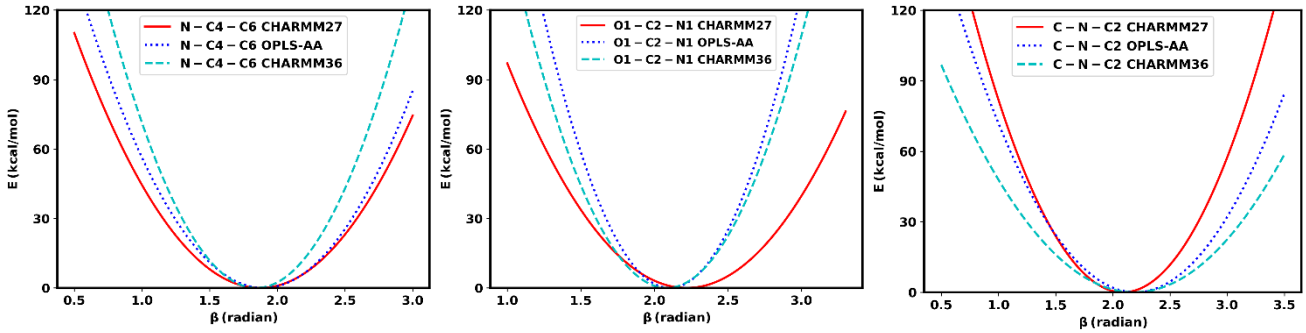

(a) Omeprazole (b) Favipiravir (c) Amoxicillin

Fig. 3: Harmonic bond angle potentials of the form $k_\beta(\beta - \beta_0)^2$ for the atom pairs of (a) omeprazole, (b) favipiravir, and (c) amoxicillin for CHARMM27 (red), OPLS-AA (blue, dotted), and CHARMM36 (cyan, dotted).

Bond angle potential is not suitable for larger deviation from equilibrium values due to atom dissociation and no longer interaction [43]. Bond geometries in molecules are reproduced by designing bond angle potentials which are controlled by atomic orbital hybridization. The bond angle potential is derived from the arrangements of covalent bonds around the atom by sp, sp^2, and sp^3 hybridization. The bond angles are distorted by the local environment [44].

Even the minute difference of (1-2)° between various bond angles has a noticeable overall impact on the molecular structure [45]. The geometry is also influenced by the ring molecules and electron lone pairs surrounding the atoms. Due to its boundness and simplicity in application and differentiation, a trigonometric function from the Taylor series is used for bond angle potential [46]. The odd power of deformation is not used because it has negative coefficients and will be hazardous for bond angle potential [47]. For a small range of fluctuation, the angular vibrational motion occurring between three atoms (i, j, and k) is explained by harmonic bond stretching potential. The potential energy increases when the angle deviates greater from the ideal value. Bond angles require less energy to distort than bond length because bending energy undergoes smaller changes than stretching energy [48]. Therefore, force constants are found usually smaller for bending than those for stretching.

Dihedral Angle Energy

The energy profiles of dihedral potentials (Figure 4-a, b, and c) showed that the sinusoidal curve was found more deviating from the equilibrium position in the selected atom groups C3-N-C4-C6 of omeprazole, N1-C3-C4-N2 of favipiravir, and C10-C9-C8-O3 of amoxicillin molecules for CHARMM27, OPLS-AA, and CHARMM36 parameters, respectively. The parameters are listed in Table 3. The characteristic flexibility of the molecules is found in energy profiles of the dihedral which are significant factors for ligand association or dissociation mechanics [49]. A key aspect of the local structure of proteins is the unfrozen dihedral potential. There is no complete understanding of the origin of dihedral potential [50].

Table 3: Parameters for dihedral angle interactions under CHARMM27, OPLS-AA, and CHARMM36 FFs

Molecule	Atoms	CHARMM27			OPLS-AA			CHARMM36		
		k_α (kcal/mol)	n	δ (degree)	k_α (kcal/mol)	n	δ (degree)	k_α (kcal/mol)	n	δ (degree)
Omeprazole	C3-N-C4-C6	2.0000	2	180	3.6250	2	180	6.0000	2	180
Favipiravir	N1-C3-C4-N2	6.0000	2	180	3.6250	2	180	1.9300	2	180
Amoxicillin	C10-C9-C8-O3	0.2000	2	180	0.2730	2	180	0.6700	2	180

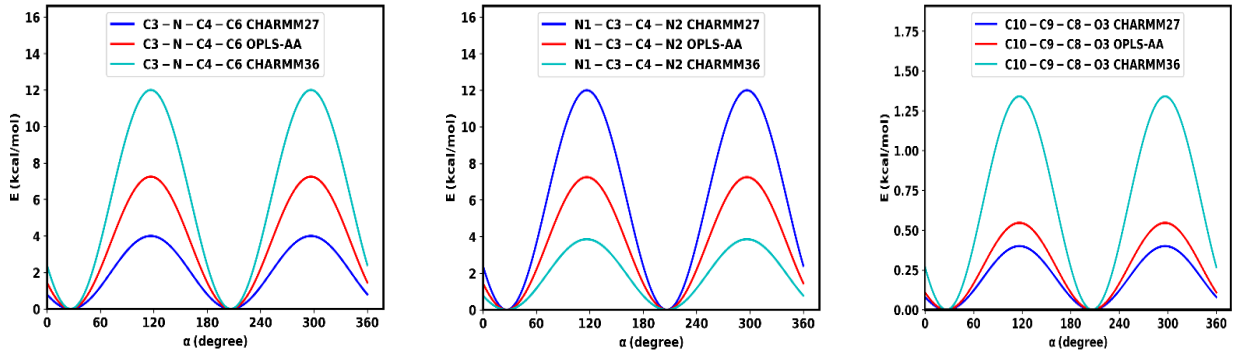

(a) Omeprazole (b) Favipiravir (c) Amoxicillin

Fig. 4: Energy profiles of two-fold dihedral angle potentials of the form $k_\propto[1+\cos(n \propto -\delta)]$ for the atom groups of (a) omeprazole, (b) favipiravir, and (c) amoxicillin for three different force fields: CHARMM27 (blue), OPLS-AA (dotted, red), and CHARMM36 (cyan).

The torsional parameter plays a vital role in the determination of molecular conformational energy which impacts the protein-ligand binding [51]. This torsional type is represented by truncated Fourier series. Fitting each torsion type to determine the associated van der Waals 1-4 parameters yields the molecular quantum chemical torsion energy profiles. The energy contribution such as bond length, bending term, and non-bonded terms are not able to sufficiently predict the torsional energy so that torsional potentials are introduced. This potential provides an explanation for the reduction of steric congestion and the best possible resonance stabilization [52].

Torsional energy is typically only significant for single bonds because double or triple bonds are too rigid to permit rotation [53]. The torsional constant k_α and α are used for one-fold rotational barriers and central bonds in the molecules. The bonds of groups attached to a central rotating bond are thought to be attracted to one another by torsional energies. Some force field adds higher-order terms in the potential functions to account for the anharmonic effects since the harmonic description is only valid for small deformations [54]. The term n indicates the number of minima in the function, the term δ determines the torsional angle, and the term α indicates the angle between the planes formed by the first and the last three of the four atoms.

When the bond rotates 360° the torsional energy should return to its initial value. The different values of n such as 1, 2, and 3 signify the 360° rotation, 180° periodicity, and 120° periodicity [55]. A cosine function is used to describe the proper torsional potentials. The optimization of the four-bodied dihedral term addresses the bond rotation and torsional energies around bonds in molecules. When the value of δ falls outside of the range of 0° and 180°, the asymmetry induction causes different energies for molecules with stereogenic centers. Because they are 100 times less stiff than bond stretching motions, torsion bonds guarantee the reproduction of significant conformational changes brought on by bond rotation and the proper level of rigidity of the molecule [56]. As a result, the local structure of the macromolecule is significantly shaped by torsional motion.

Lennard-Jones Energy

Attractive forces are produced by cross-correlated motions of electrons in neighboring non-bonded terms, whereas repulsive forces are produced by electron's inability to occupy the same orbitals due to Pauli exclusion [57]. Lennard-Jones 6-12 potentials are used to calculate the interaction of atoms i and j in different residues [58]. There are overlapped repulsive parts at shorter distances and overlapped attractive parts at longer distances for the selected atom pairs of the molecules. The curves are observed to be distinct at about the intermediate distance 2 Å due to the different values of well-depth parameters (ϵ_{ij}) as shown in Figures 5-a, b and c.

Table 4: Parameters for Lennard-Jones potential interactions under CHARMM27, and OPLS-AA FFs

Molecule	Atoms	CHARMM27		OPLS-AA	
		ϵ_{ij} (kcal/mol)	σ_{ij} (Å)	ϵ_{ij} (kcal/mol)	σ_{ij} (Å)
Omeprazole	O1	-0.120000	1.700000	-0.170000	1.661244
Favipiravir	O1	-0.120000	1.700000	-0.210000	1.661244
Amoxicillin	O3	-0.120000	1.700000	-0.210000	1.661244

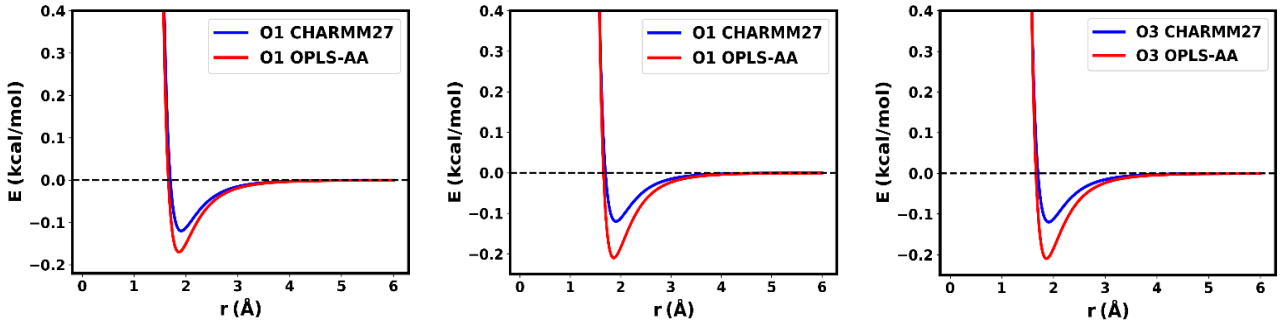

(a) Omeprazole (b) Favipiravir (c) Amoxicillin

Fig. 5: Energy profiles of van der Waals interaction of the form $4\epsilon_{ij}\left[\left(\frac{\sigma_{ij}}{r_{ij}}\right)^{12} - \left(\frac{\sigma_{ij}}{r_{ij}}\right)^{6}\right]$ for atom pairs of (a) omeprazole, (b) favipiravir, and (c) amoxicillin for three different force fields: CHARMM27 (blue), OPLS-AA (red)

Lennard-Jones potentials take into account the long-range van der Waals attractive forces and the short-range Pauli repulsion forces [59]. Although the Lennard-Jones force is zero at the cutoff, the cutoff scheme has an effect on the overall potential. When two interacting atoms are near an optimal internuclear distance, they attract one another; however, when they are very close, they repel one another. The steep repulsion experienced by electron clouds when they interact has a quantum origin because it is affected by the Pauli-exclusion principle [60].

This interaction is crucial in determining the 3-D structure of many biomolecules. The repulsive forces are the most important in determining the shape of molecules. The van der Waals radius is used to measure the size of an atom because it is the distance that gives the lowest, most favorable energy of interaction between two atoms [61]. In this potential, the term r^{-12} accounts for the short-range repulsion whereas the term r^{-6} accounts for the London dispersion attraction. The potential is truncated to zero more rapidly by using cut-off distances as it goes to zero as r_{ij} increases so that the computational efficiency is found to increase [62].

A mild attraction between electron clouds due to electron-electron correlation is found at intermediate states [63]. The travel of the electrons through the molecule, which affects the nearby molecule, induces a dipole-dipole moment that attracts two atoms [64] . The dipole-quadrupole and quadrupole-quadrupole interactions between two fragments are neglected because they do not have a

high contribution to the overall energy. The corresponding well depth of the interaction between two atoms i and j is given by the geometric mean $\epsilon_{ij} = (\epsilon_i \epsilon_j)^{\frac{1}{2}}$ for Lennard-Jones potential. Depending upon the force field chosen, the arithmetic mean $\sigma_{ij} = \frac{1}{2}(\sigma_i + \sigma_j)$ and geometric mean $\sigma_{ij} = (\sigma_i \sigma_j)^{\frac{1}{2}}$ gives the values at which potential becomes zero (i.e. distance at which repulsive and attractive terms balance out [65] . The energy of the system rises as long as there is no possibility of bonding.

Electrostatic Energy

The distributions of end-to-end distances of S-C1 of omeprazole, C1-C3 of favipiravir, and O3-C9 of amoxicillin were found more skewed under CHARMM27, OPLS-AA, and CHARMM36 parameters as shown in Figure 6-a, b, and c. The generated parameters for the electrostatic interactions have been presented in Table 5.

Table 5: Parameters for electrostatic interactions under CHARMM27, OPLS-AA, and CHARMM36 FFs

		CHARMM27				OPLS-AA				CHARMM36			
Molecule	Atoms	q_i	q_j	ϵ_r	K	q_i	q_j	ϵ_r	K	q_i	q_j	ϵ_r	K
		$(q_i \cdot e^-)$	$(q_j \cdot e^-)$			$(q_i \cdot e^-)$	$(q_j \cdot e^-)$			$(q_i \cdot e^-)$	$(q_j \cdot e^-)$		
Omeprazole	S * C1	0.2955	0.1665	5	332	0.8667	0.1216	5	332	0.2820	0.0360	5	332
Favipiravir	C1 * C3	0.4500	-0.0410	5	332	-0.0594	0.0708	5	332	-0.3890	0.1090	5	332
Amoxycilin	O3 * C9	-0.5700	0.4745	5	332	-0.3986	0.1335	5	332	-0.5400	0.3310	5	332

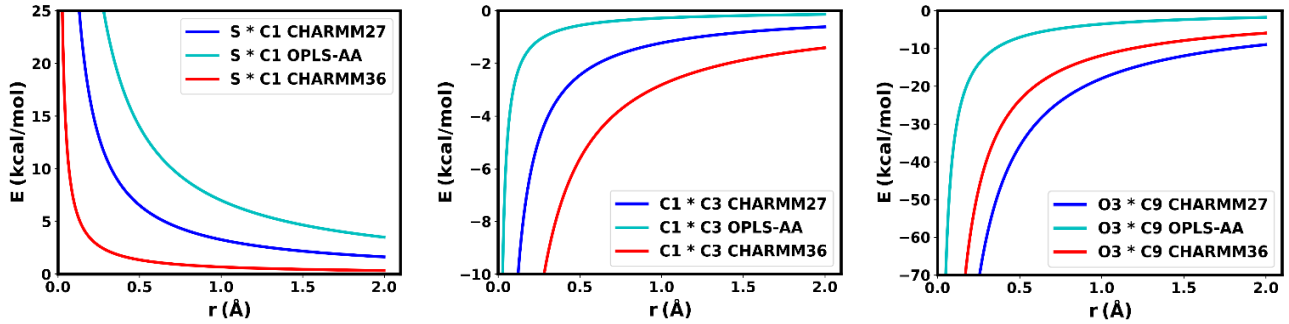

(a) Omeprazole (b) Favipiravir (c) Amoxicillin

Fig. 6: Energy profiles of electrostatic interactions of the form $\frac{Kq_iq_j}{\epsilon_{rij}}$ different atom pairs of (a) omeprazole, (b) favipiravir, and (c) amoxicillin for CHARMM27 (blue), OPLS-AA (cyan), and CHARMM36 (red).

Water (dielectric constant = 80) plays a vital role in the effective screening of electrostatic interactions due to which this potential decays faster than $1/r$ [66]. This interaction is called long-ranged as it decays as r^{-1} . The skewness of electrostatic nature is directly proportional to the magnitude of partial charges of the corresponding atom pair. The slowly declining electrostatic contribution is provided by the inverse of distance outside the cut-off distance [67]. The potential is modulated to maintain continuity around the cut-off distance.

The goal of ab-initio or quantum mechanical calculations is to obtain well-founded partial charges. Because atomic charges are not experimentally observable, different methods do not always produce the same distribution of partial charges [68]. For practical reasons and computational efficiency, partial charges are normally assigned in atomic sites. It is also thought that the rotational barrier is determined by the specific combination of dihedral potential with electrostatic and 1-4 van der Waals interactions [69]. Therefore, it will not be true to combine parameters or modify them coming from different sources. Coulomb's law approximates the ionic interactions between fully and partially charged groups for each atom pair. The partial electrostatic charges are found residing on the atoms when the bonds in the molecule are polar. The polarizable

force field is needed to be employed for highly polarizable groups or ions as the electrostatic term becomes less accurate for these groups. The Coulomb approach is sufficient for organic systems such as proteins [70].

The results produced by the CGenFF, SwissParam, and LigParGen force fields are generally consistent with the results of the experiment; however, the inconsistent protein-ligand and solvent-ligand interactions observed during molecular simulations are caused by the changing topology and parameters. The results emphasize the importance of correctly assigning partial charges and van der Waals parameters to non-bonded interactions in order to develop quantitatively accurate models of intermolecular interactions [71]. The default parameters that the CGenFF server generates at least in our hands certainly need additional refining. These servers are very valuable for academics interested in using molecular mechanics simulations to examine any phenomenon dependent on intermolecular interactions with ligands. The force field parameters, including the force constants K, are generated based on various factors such as the specific atoms and functional groups present in the molecule being studied, as well as the type of interactions between these atoms and groups. The differences in the parameters generated by different servers like Swissparam, LigParGen, and CGenFF may be due to variations in the methods and algorithms used to calculate these parameters. Each of these force fields has its strengths and weaknesses, so ultimately it will depend on our specific research needs. CHARMM27 is an older force field that is still widely used due to its accuracy in reproducing experimental observations. However, CHARMM36 is a newer and more advanced force field that is better suited for simulations of complex biomolecules. Lamichhane et al. used CHARMM27 as well as CHARMM36 force fields to parameterize small molecules like hormones and drugs, and also used to perform NAMD simulations of protein-ligand systems [72-75]. OPLS-AA, on the other hand, has been specifically designed for small molecules and is often used in drug design studies. Ultimately, the best force field for our research depend on the type of molecules we are studying and the specific questions we are trying to answer.

CONCLUSION

Based on the comparative analysis, it can be concluded that both bonded and non-bonded force fields have their strengths and weaknesses when it comes to analyzing drug-like molecules. Bonded force fields are suitable for modeling smaller molecules with simple structures while non-bonded force fields are better suited for larger and more complex molecules. However, a combination of both force fields can provide more accurate predictions of the behavior of drug molecules in biological systems. Ultimately, the choice of force field should be based on the specific properties and characteristics of the drug-like molecule being studied. Topology and parameters of small drug-like molecules such as omeprazole, favipiravir, and amoxicillin were obtained using force field optimization under the SwissParam, LigParGen, and CGenFF programs in order to analyze the variation of energy profiles of bonded and non-bonded terms of the potential function. Despite the differences in the drawn energy profiles of these molecules, it is expected that they will agree well with the experimental results. The widely varying topology and parameters may result in inconsistencies in molecular simulation results. Because all force fields produce better results for aliphatic groups than aromatic groups, aromatic molecule treatment needs to be improved. The bond length and bond angle energies are found to be minimum at the reference values. Depending on the generated parameters, slightly deviating parabolic potential curves are produced. The same atom pair exhibits different characteristic flexibility which will be important for ligand association and dissociation during MD simulations. Due to its lower stiffness than bond length interaction, dihedral energy profiles have undergone significant changes. The attractive parts at longer distances and the repulsive parts at shorter distances in Lennard-Jone's potential curves have been found to overlap. Due to varying values of the well-depth parameters, the curves at about 2Å distance appear distinct. The electrostatic curve resulting from the partial charges of non-bonded atoms decays exponentially and has no cut-off distances. It has been discovered that the greater magnitude of the partial charges is what causes the higher skewness at end-to-end distances. Because both the bond and angle terms use the harmonic function, a quick examination of the potential functions under CHARMM27, OPLS-AA, and CHARMM36 reveals similarity for both terms. The interactions caused by compressing or stretching bonds beyond their equilibrium lengths and angles, torsional effects of twisting about single bonds, van der Waals attractions or repulsion between atoms that come close together, and

electrostatic interactions between partial charges due to polar bonds are all responsible for a molecule's steric energy. This study will be helpful to figure out a way to evaluate and enhance the force field performance.

DECLARATIONS

Ethical Issue

The authors declare that they have no ethical issues related to this research.

Competing Interests

The authors declare that they have no competing interests of a financial or personal nature.

Author Contributions

PKY prepared structures and analyzed the data. TRL designed the research. PKY and TRL wrote the article.

Funding

Not applicable.

Data Availability

The data supporting the findings are available in the supplementary file.

REFERENCES

[1] Hospital, A.; Goñi, J. R.; Orozco, M. and Gelpí, J. L. Molecular dynamics simulations: advances and applications. *Journal of Advances and* Applications *in Bioinformatics and Chemistry*, 37-47 (2015).

[2] MacKerell Jr, A. D. Empirical force fields for biological macromolecules: overview and issues. *Journal of computational Chemistry*, **25** (13): 1584-1604 (2004).

[3] Gohlke, H. and Klebe, G. Approaches to the description and prediction of the binding affinity of small-molecule ligands to macromolecular receptors. *Journal of Angewandte Chemie International Edition*, **41** (15): 2644-2676 (2002).

[4] Jorgensen, W. L. and Tirado-Rives, J. The OPLS [optimized potentials for liquid simulations] potential functions for proteins, energy minimizations for crystals of cyclic peptides and crambin. *Journal of the American Chemical Society*, **110** (6): 1657-1666 (1988).

[5] Dodda, L. S.; Vilseck, J. Z.; Cutrona, K. J. and Jorgensen, W. L. Evaluation of CM5 charges for nonaqueous condensed-phase modeling. *Journal of Chemical Theory and Computation*, **11** (9): 4273-4282 (2015).

[6] Udier–Blagović, M.; Morales De Tirado, P.; Pearlman, S. A. and Jorgensen, W. L. Accuracy of free energies of hydration using CM1 and CM3 atomic charges. *Journal of Computational Chemistry*, **25** (11): 1322-1332 (2004).

[7] Vanommeslaeghe, K. and MacKerell Jr, A. D. Automation of the CHARMM General Force Field (CGenFF) I: bond perception and atom typing. *Journal of Chemical Information and Modeling*, **52** (12): 3144-3154 (2012).

[8] Klimovich, P. V. and Mobley, D. L. Predicting hydration free energies using all-atom molecular dynamics simulations and multiple starting conformations. *Journal of Computer-Aided Molecular Design*, **24** (12): 307-316 (2010).

[9] Shirts, M. R. and Pande, V. S. Solvation free energies of amino acid side chain analogs for common molecular mechanics water models. *The Journal of Chemical Physics*, **122** (13): 134508 (2005).

[10] Dodda, L. S.; de Vaca, I.; Tirado-Rives, J. and Jorgensen, W. L. LigParGen web server: an automatic OPLS-AA parameter generator for organic ligands. *Journal of Nucleic Acids Research*, **45** (W1): W331–W336 (2017).

[11] Šponer, J.; Banáš, P.; Jurecka, P.; Zgarbová, M.; Kührová, P.; Havrila, M.; Krepl, M.; Stadlbauer, P. and Otyepka, M. Molecular dynamics simulations of nucleic acids. From tetranucleotides to the ribosome. *The Journal of Physical Chemistry Letters*, **5** (10): 1771-1782 (2014).

[12] Leach, A. R. Molecular modelling: principles and applications, Pearson Education (2001).

[13] Van Der Spoel, D.; Lindahl, E.; Hess, B.; Groenhof, G.; Mark, A. E. and Berendsen, H. J. C. GROMACS: fast, flexible, and free. *Journal of Computational Chemistry*, **26** (16): 1701-1718 (2005).

[14] Rao, P.; Shukla, A.; Parmar, P.; Rawal, R. M.; Patel, B.; Saraf, M. and Goswami, D. Reckoning a fungal metabolite, Pyranonigrin A as a potential Main protease (Mpro) inhibitor of novel SARS-CoV-2 virus identified using docking and molecular dynamics simulation. *Journal of Biophysical Chemistry*, **264**: 106425 (2020).

[15] Halgren, T. A. Merck molecular force field. I. Basis, form, scope, parameterization, and performance of MMFF94. *Journal of Computational Chemistry*, **17** (5-6): 490-519 (1996).

[16] Sonibare, K.; Rathnayaka, L. and Zhang, L. Comparison of CHARMM and OPLS-aa forcefield predictions for components in one model asphalt mixture. *Journal of Construction and Building Materials*, **236**: 117577 (2020).

[17] Zoete, V.; Cuendet, M. A.; Grosdidier, A. and Michielin, O. SwissParam: a fast force field generation tool for small organic molecules.

Journal of Computational Chemistry, **32**(11): 2359-2368 (2011).

[18] Grosdidier, A.; Zoete, V. and Michielin, O. SwissDock, a protein-small molecule docking web service based on EADock DSS. *Nucleic Acids Research*, **39** (suppl_2): W270–W277 (2011).

[19] Zhu, X.; Lopes, P. E. M. and MacKerell Jr, A. D. Recent developments and applications of the CHARMM force fields. *Wiley Interdisciplinary Reviews: Computational Molecular Science*, **2** (1): 167-185 (2012).

[20] Heinzmann, T. Force Field Development of β-lactam Class Antibiotics. *SMU Journal of Undergraduate Research*, **5** (1): 2 (2020).

[21] Roos, K.; Wu, C.; Damm, W.; Reboul, M.; Stevenson, J. M.; Lu, C.; Dahlgren, M. K.; Mondal, S.; Chen, W.; Wang, L. et al. OPLS3e: Extending force field coverage for drug-like small molecules. *Journal of Chemical Theory and Computation*, **15** (3): 1863-1874 (2019).

[22] Darden, T. A. Treatment of long-range forces and potential. *Journal of Computational Biochemistry and Biophysics*, pages 103-126. CRC Press, (2001).

[23] Adcock, S. A. and McCammon, J. A. Molecular dynamics: survey of methods for simulating the activity of proteins. *Journal of Chemical Reviews*, **106** (5): 1589-1615 (2006).

[24] Lerbret, A.; Affouard, F.; Bordat, P.; Hédoux, A.; Guinet, Y. and Descamps, M. Molecular dynamics simulations of lysozyme in water/sugar solutions. *Journal of Chemical Physics*, **345** (2-3): 267-274 (2008).

[25] Momany, F. A.; McGuire, R. F.; Burgess, A. W. and Scheraga, H. A. Energy parameters in polypeptides. VII. Geometric parameters, partial atomic charges, nonbonded interactions, hydrogen bond interactions, and intrinsic torsional potentials for the naturally occurring amino acids. *The Journal of Physical Chemistry*, **79** (22): 2361-2381 (1975).

[26] Jones, J. E. On the determination of molecular fields.—II. From the equation of state of a gas. *Proceedings of the Royal Society of London. Series A, Containing Papers of a Mathematical and Physical Character*, **106** (738): 463-477 (1924).

[27] Madjet, M. E.; Abdurahman, A. and Renger, Th. Intermolecular Coulomb couplings from ab initio electrostatic potentials: application to optical transitions of strongly coupled pigments in photosynthetic antennae and reaction centers. *The Journal of Physical Chemistry B*, **110** (34): 17268-17281 (2006).

[28] Phillips, J. C.; Braun, R.; Wang, W.; Gumbart, J.; Tajkhorshid, E.; Villa, E.; Chipot, C.; Skeel, R. D.; Kale, L. and Schulten, K. Scalable molecular dynamics with NAMD. *Journal of Computational Chemistry*, **26** (16): 1781-1802 (2005).

[29] Mayne, C. G.; Saam, J.; Schulten, K.; Tajkhorshid, E. and Gumbart, J. C. Rapid parameterization of small molecules using the force field toolkit. *Journal of Computational Chemistry*, **34** (32): 2757-2770 (2013).

[30] Vanommeslaeghe, K.; Hatcher, E.; Acharya, C.; Kundu, S.; Zhong, S.; Shim, J.; Darian, E.; Guvench, O.; Lopes, P.; Vorobyov, I. et al. CHARMM general force field: A force field for drug-like molecules compatible with the CHARMM all-atom additive biological force fields. *Journal of Computational Chemistry*, **31** (4): 671-690 (2010).

[31] Schleif, R. A concise guide to CHARMM and the analysis of protein structure and function. *WWW*, (2013).

[32] REIHER III, W. H. Theoretical studies of hydrogen bonding. *Ph. D. Thesis at Harvard University* (1985).

[33] Mackerell Jr, A. D.; Feig, M. and Brooks III, C. L. Extending the treatment of backbone energetics in protein force fields: Limitations of gas-phase quantum mechanics in reproducing protein conformational distributions in molecular dynamics simulations. *Journal of Computational Chemistry*, **25** (11): 1400-1415 (2004).

[34] MacKerell Jr, A. D.; Banavali, N. and Foloppe, N. Development and current status of the CHARMM force field for nucleic acids. *Journal of Biopolymers: Original Research on Biomolecules*, **56** (4): 257-265 (2000).

[35] Dauber-Osguthorpe, P. and Hagler, A. T. Biomolecular force fields: where have we been, where are we now, where do we need to go and how do we get there? *Journal of computer-aided molecular design*, **33** (2): 133-203 (2019).

[36] Mottin, M.; Souza, P. C. T.; Ricci, C. G. and Skaf, M. S. CHARMM Force Field Parameterization of Peroxisome Proliferator-Activated Receptor γ Ligands. *International Journal of Molecular Sciences*, **18** (1): 15 (2016).

[37] Broyden, C. G. Quasi-Newton, or modification methods. In: *Numerical Solution of Systems of Nonlinear Algebraic Equations*, Elsevier, 241-280 (1973).

[38] Hanson, R. M.; Prilusky, J.; Renjian, Z.; Nakane, T. and Sussman, J. L. JSmol and the next-generation web-based representation of 3D molecular structure as applied to proteopedia. *Israel Journal of Chemistry*, **53** (3-4): 207-216 (2013).

[39] González, M. A. Force fields and molecular dynamics simulations. *École thématique de la*

Société Française de la Neutronique, **12**: 169-200 (2011).

[40] Grimme, S. A general quantum mechanically derived force field (QMDFF) for molecules and condensed phase simulations. *Journal of Chemical Theory and Computation*, **10** (10): 4497-4514 (2014).

[41] Comba, P.; Hambley, T. W. and Martin, B. Molecular modeling of inorganic compounds. John Wiley & Sons (2009).

[42] Brenner, D. W.; Shenderova, O. A.; Harrison, J. A.; Stuart, S. J.; Ni, B. and Sinnott, S. B. A second-generation reactive empirical bond order (REBO) potential energy expression for hydrocarbons. *Journal of Physics: Condensed Matter*, **14** (4): 783 (2002).

[43] Van Duin, A. C. T.; Dasgupta, S.; Lorant, F. and Goddard, W. A. ReaxFF: a reactive force field for hydrocarbons. *The Journal of Physical Chemistry A*, **105** (41): 9396-9409 (2001).

[44] Małolepsza, E.; Strodel, B.; Khalili, M.; Trygubenko, S.; Fejer, S. N. and Wales, D. J. Symmetrization of the AMBER and CHARMM force fields. *Journal of Computational Chemistry*, **31** (7): 1402-1409 (2010).

[45] Krieger, E.; Joo, K.; Lee, J.; Lee, J.; Raman, S.; Thompson, J.; Tyka, M.; Baker, D. and Karplus, K. Improving physical realism, stereochemistry, and side-chain accuracy in homology modeling: Four approaches that performed well in CASP8. *Journal of Proteins: Structure, Function, and Bioinformatics*, **77** (S9): 114-122 (2009).

[46] Bond-Taylor, S.; Leach, A.; Long, Y. and Willcocks, C. G. Deep generative modelling: A comparative review of VAEs, GANs, normalizing flows, energy-based and autoregressive models. *arXiv preprint arXiv:2103.04922*, (2021).

[47] Thomas, S. and Lee, S. U. Atomistic insights into the anisotropic mechanical properties and role of ripples on the thermal expansion of h-BCN monolayers. *Journal of RSC Advances*, **9** (3): 1238-1246 (2019).

[48] Abagyan, R.; Totrov, M. and Kuznetsov, D. ICM—A new method for protein modeling and design: Applications to docking and structure prediction from the distorted native conformation. *Journal of Computational Chemistry*, **15** (5): 488-506 (1994).

[49] Hansson, A.; Souza, P. C. T.; Silveira, R. L.; Martínez, L. and Skaf, M. S. CHARMM force field parameterization of rosiglitazone. *International Journal of Quantum Chemistry*, **111** (7-8): 1346-1354 (2011).

[50] Skolnick, J. In quest of an empirical potential for protein structure prediction. *Journal of Current Opinion in Structural Biology*, **16** (2): 166-171 (2006).

[51] Huang, N.; Kalyanaraman, C.; Bernacki, K. and Jacobson, M. P. Molecular mechanics methods for predicting protein–ligand binding. *Journal of Physical Chemistry Chemical Physics*, **8** (44): 5166-5177 (2006).

[52] Engler, E. M.; Andose, J. D. and Schleyer, P. V. R. Critical evaluation of molecular mechanics. *Journal of the American Chemical Society*, **95** (24): 8005-8025 (1973).

[53] Allinger, N. L.; Yuh, Y. H. and Lii, J. H. Molecular mechanics. The MM3 force field for hydrocarbons. *Journal of the American Chemical Society*, **111** (23): 8551-8566 (1989).

[54] Császár, A. G. Anharmonic molecular force fields. *Wiley Interdisciplinary Reviews: Computational Molecular Science*, **2** (2): 273-289 (2012).

[55] Fan, C. F.; Cagin, T.; Shi, W. and Smith, K. A. Local chain dynamics of a model polycarbonate near glass transition temperature: A molecular dynamics simulation. *Journal of Macromolecular Theory and Simulations*, **6** (1): 83-102 (1997).

[56] Xiao, M.; Carey, R. L.; Chen, H.; Jiao, X.; Lemaur, V.; Schott, S.; Nikolka, M.; Jellett, C.; Sadhanala, A.; Rogers, S. et al. Charge transport physics of a unique class of rigid-rod conjugated polymers with fused-ring conjugated units linked by double carbon-carbon bonds. *Journal of Science Advances*, **7** (18): eabe5280 (2021).

[57] Alford, R. F.; Leaver-Fay, A.; Jeliazkov, J. R.; O'Meara, M. J.; DiMaio, F. P.; Park, H.; Shapovalov, M. V.; Renfrew, P. D.; Mulligan, V. K.; Kappel, K. et al. The Rosetta all-atom energy function for macromolecular modeling and design. *Journal of Chemical Theory and Computation*, **13** (6): 3031-3048 (2017).

[58] Park, H.; Bradley, P.; Greisen, P. Jr.; Liu, Y.; Mulligan, V. K.; Kim, D. E.; Baker, D. and DiMaio, F. Simultaneous optimization of biomolecular energy functions on features from small molecules and macromolecules. *Journal of Chemical Theory and Computation*, **12** (12): 6201-6212 (2016).

[59] Néel, N. and Kröger, J. Atomic force extrema induced by the bending of a CO-functionalized probe. *Journal of Nano Letters*, **21** (5): 2318-2323 (2021).

[60] Wilson, A. L. and Popelier, P. L. A. Exponential relationships capturing atomistic short-range repulsion from the interacting quantum atoms (IQA) method. *The Journal of Physical Chemistry A*, **120** (48): 9647-9659 (2016).

[61] Mantina, M.; Chamberlin, A. C.; Valero, R.; Cramer, C. J. and Truhlar, D. G. Consistent van der Waals radii for the whole main group. *The Journal of Physical Chemistry A*, **113** (19): 5806-5812 (2009).

[62] Šponer, J.; Šponer, J. E.; Mládek, A.; Jurečka, P.; Banáš, P. and Otyepka, M. Nature and magnitude of aromatic base stacking in DNA and RNA: Quantum chemistry, molecular mechanics, and experiment. *Journal of Biopolymers*, **99** (12): 978-988 (2013).

[63] Rick, S. W. and Stuart, S. J. Potentials and algorithms for incorporating polarizability in computer simulations. *Reviews in Computational Chemistry*, **18**: 89-146 (2002).

[64] Badenhoop, J. K. and Weinhold, F. Natural steric analysis: Ab initio van der Waals radii of atoms and ions. *The Journal of Chemical Physics*, **107** (14): 5422-5432 (1997).

[65] Roux, B. *Computational Modeling and Simulations of Biomolecular Systems***, World Scientific (2021).

[66] Gunner, M. R.; Nicholls, A. and Honig, B. Electrostatic potentials in Rhodopseudomonas viridis reaction centers: implications for the driving force and directionality of electron transfer. *The Journal of Physical Chemistry*, **100** (10): 4277-4291 (1996).

[67] Deserno, M. and Holm, C. How to mesh up Ewald sums. I. A theoretical and numerical comparison of various particle mesh routines. *The Journal of Chemical Physics*, **109** (18): 7678-7693 (1998).

[68] Sigfridsson, E. and Ryde, U. Comparison of methods for deriving atomic charges from the electrostatic potential and moments. *Journal of Computational Chemistry*, **19** (4): 377-395 (1998).

[69] Cornell, W. D.; Cieplak, P.; Bayly, C. I.; Gould, I. R.; Merz, K. M.; Ferguson, D. M.; Spellmeyer, D. C.; Fox, T.; Caldwell, J. W. and Kollman, P. A. A second generation force field for the simulation of proteins, nucleic acids, and organic molecules. *Journal of the American Chemical Society*, **117** (19): 5179-5197 (1995).

[70] Allinger, N. L.; Yuh, Y. H. and Lii, J. H. Molecular mechanics. The MM3 force field for hydrocarbons. *Journal of the American Chemical Society*, **111** (23): 8551-8566 (1989).

[71] Zhu, S. Validation of the generalized force fields GAFF, CGenFF, OPLS-AA, and PRODRGFF by testing against experimental osmotic coefficient data for small drug-like molecules. *Journal of Chemical Information and Modeling*, **59** (10): 4239-4247 (2019).

[72] Lamichhane, T. R. and Lamichhane, H. P. Heat conduction by thyroid hormone receptors. *AIMS Biophysics*, **5** (4): 245-256 (2018).

[73] Lamichhane, T. R.; Paudel, S.; Yadav, B. K. and Lamichhane, H. P. Echo dephasing and heat capacity from constrained and unconstrained dynamics of triiodothyronine nuclear receptor protein. *Journal of Biological Physics*, **45**: 107-125 (2019).

[74] Lamichhane, T. R. and Lamichhane, H. P. Structural changes in thyroid hormone receptor-beta by T3 binding and L330S mutational interactions. *AIMS Biophysics*, **7** (1): 27-40 (2020).

[75] Lamichhane, T. R. and Ghimire, M. P. Evaluation of SARS-CoV-2 main protease and inhibitor interactions using dihedral angle distributions and radial distribution function. *Heliyon*, **7** (10): e08220 (2021).